



## STUDYING AND SIMULATING THE INFLUENCE OF THE ROTOR FAULT ON STATOR CURRENT

**Katalin ÁGOSTON**

*University of Medicine, Pharmacy, Science and Technology "G.E. Palade" of Tîrgu Mureș  
Nicolae Iorga Street, no. 1, 540088, Mureș Country, Romania  
katalin.agoston@umfst.ro*

### Abstract

*This paper presents fault detection techniques, especially the motor current signature analysis (MCSA) which consists of the phase current measurement of the electrical motor's stator and/or rotor. The motor current signature analysis consists in determining the frequency spectrum (FFT) of the stator current signal and evaluating the relative amplitude of the current harmonics. Sideband frequencies appear in the frequency spectrum of the current, corresponding to each fault. The broken bar is a frequent fault in induction motors with squirrel-cage rotor. It is presented the equivalent circuit for induction motors and the equivalence between the squirrel-cage rotor and the rotor windings. It is also presented an equivalent circuit model for induction motors with squirrel cage rotor, and based on this a Simulink model was developed. It is shown how a broken rotor bar influences the magnetic field around the rotor and through this the stator current. This modification is highlighted through the developed model.*

**Key words:** motor fault detection, simulation, motor model, equivalent circuit

### 1. Introduction

Induction motors are present in almost all equipments and the motor reliability influences the whole system working. Electrical motors and the other components of the systems are bound in different ways and react in different manner to external forces.

During operation electrical and mechanical systems produce noise and vibrations. Vibrations caused by motors and other equipments propagate in the environment and influence the operation of other systems. Unwanted vibrations lead to mechanical usage, or electrical breakdowns. Vibrations are due to imbalanced or misaligned components, corroded, deformed or broken parts etc. These irregularities can appear during operation due to the influence of the environment (temperature, pressure, humidity,

corrosive air, etc.) or can be present from assembling and during operation they can get worse.

Furthermore induction motors are consumers of electrical power and they consume more than 50% of the total electricity produced. For this reason they are very important and their control and reliability are improving. The sooner the faults are detected the better and faster one can intervene to solve the problem and reduce the losses. This motivates the development of faster and more trustworthy maintenance and control techniques.

Knowing the most important faults and having the proper fault detection technique, the problem can be solved without spending time and money. [1][2]

The fault detection techniques can be classified in model-based techniques and signal-based techniques.

The model-based techniques use mathematical expressions which describe the relationship between the electrical motor's parameters at normal, ideal functioning condition. By introducing disturbances in these models the equations become complicated and hard to use.

The signal-based techniques use different measured signals (vibration or current) using different sensors and transducers (accelerometers, current transducers). Through these signals the electrical motor condition can be estimated. In this case it is also required the acquisition of signals which describe the normal function, and to which the further measurement signals are compared. The signal-based techniques use time-domain analysis, frequency-domain analysis and time-frequency analysis. [3]

One of the signal-based techniques is the motor current signature analysis (MCSA), which uses the phase current measurement and analysis of the electrical motor's stator and/or rotor. But a simple overcurrent and/or overvoltage detection by electrical motors is not enough to predict the fault. In this case the motor must be disconnected and the fault must be examined.

A continuous surveillance of the electrical motor parts using different methods allows an early detection of an incipient fault. The shutdown of the motor cannot be avoided, but shutdown time can be reduced and serious consequences also.

## 2. Motor current signature analysis

The motor current signature analysis (MCSA) involves the monitoring and analysis of the current signal, and its characteristics which indicate the normal or abnormal motor condition. The MCSA techniques can be used to detect rotor asymmetry, stator winding error, broken bar, bearing faults and air-gap eccentricity. [3]

Motor current is influenced also by electric supply, load condition, electrical and mechanical noise, faults, so to detect a certain type of defect a lot of measurements and different types of analysis techniques are required.

The motor current signature analysis consists in determining the frequency spectrum (FFT) of the stator current signal and evaluating the relative amplitude of the current harmonics.

Specific to each fault sideband frequencies appear in the frequency spectrum. These depend on the slip and the number of pole pairs of the motor.

In [4] and [5] it is shown that the sideband frequencies due to broken bars appear at  $f_1(1\pm 2s)$ , where  $f_1$  is the motor rotation frequency and  $s$  is the slip. The rotation frequency can be calculated from the synchronism speed  $\omega_1$  and depend on the number of poles  $p$ ,  $\omega_1 = 2\pi f_1/p$  [rot/s]. If the amplitude of these harmonics exceeds a certain value in relation to the fundamental frequency a fault can be estimated. The

existence of the fault can be detected by evaluating the amplitude of the fifth harmonic  $f_1(5-4s)$  and  $f_1(5-6s)$ . The mechanical load affects the slip and so the sideband frequencies. The probability of the fault is influenced by the number of pole pairs.

The different motor faults induce different sideband frequencies which can be expressed through equations and require a good knowledge of the motor.

Analysing the harmonics' amplitude leads to a good result in case of the high power motors under constant load. At variable speed, low load torque or low power motors the amplitude of the harmonics is small and difficult to detect. If the slip is low, the sideband frequencies are close to the fundamental frequency so a high frequency resolution is needed. [4], [6]

## 3. Induction motor equivalent circuit

The induction motor modeling and simulation are commonly used methods to study and develop control systems. Dynamic model is developed through differential equations which suppose that stator and rotor windings are symmetric and the emf (electromagnetic field) is also sinusoidally distributed.

The general voltage equations for stator windings:

$$\begin{aligned} u_{1a} &= i_{1a}R_{1a} + \frac{d\Phi_{1a}}{dt} \\ u_{1b} &= i_{1b}R_{1b} + \frac{d\Phi_{1b}}{dt} \\ u_{1c} &= i_{1c}R_{1c} + \frac{d\Phi_{1c}}{dt} \end{aligned} \quad (1)$$

Where  $\Phi_i$  are the total fluxes of each stator phases including the main flux of the windings, the mutual and the leakage flux.  $R_i$  are the stator windings resistance and  $i_i$  are the stator currents. Similar equations can be written for the rotor also. [7], [8]

The self-phase inductance can be defined with the flux, which have main and leakage components too. Considering these leakage inductances and the analogy between the phases, the equations for stator and rotor can be written as following:

$$\begin{aligned} u_1(t) &= R_1 i_1 + L_{\sigma 12} \frac{di_1}{dt} + w_1 k_{w1} \frac{d\Phi_u}{dt} \\ 0 &= R_2 i_2 + L_{\sigma 21} \frac{di_2}{dt} - w_2 k_{w2} \frac{d\Phi_u}{dt} \end{aligned} \quad (2)$$

Where  $R_1, R_2$  are the stator and rotor resistances,  $L_{\sigma 12}, L_{\sigma 21}$  are the leakage inductances,  $\Phi_u$  is the useful magnetic flux,  $w_1, w_2$  are the numbers of turns of the stator and rotor windings. The rotor windings are short-circuited. [9]

Expressing these equations in complex form and reducing the rotor circuit to the stator one, the equations become:

$$\begin{aligned} \underline{U}_1 &= R_1 \underline{I}_1 + jX_{\sigma 12} \underline{I}_1 - \underline{E}_1 \\ 0 &= \frac{R'_2}{s} \underline{I}'_2 + jX'_{\sigma 12} \underline{I}'_2 + \underline{E}'_2 \end{aligned} \quad (3)$$

Where  $R'_2 = R_2 k_E^2$ ,  $X'_{\sigma 12} = X_{\sigma 21} k_E^2$ ,  $I'_2 = I_2 \frac{1}{k_E}$  and  $k_E = \frac{w_1 k_{w1}}{w_2 k_{w2}}$ ,  $\underline{E}_1 = -j2\pi f_1 w_1 k_{w1} \frac{\Phi_{max}}{\sqrt{2}}$ .

The relation between the currents:

$$\underline{I}_1 - \underline{I}'_2 = \underline{I}_{10} \quad (4)$$

The equivalent circuit for the induction motor is presented on figure 1. [10]

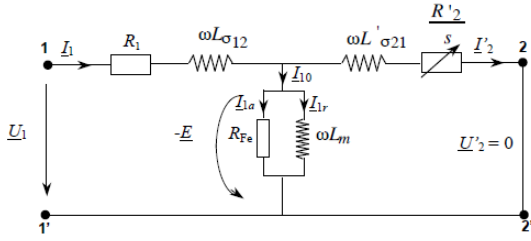


Fig.1. The equivalent circuit for an ac motor.

In case of squirrel-cage rotor the windings are replaced with conducting bars embedded in the rotor iron. The conducting bars are short-circuited at each end of the rotor by conducting rings.

The squirrel-cage rotor and winding rotor can be equal if the phase number  $m_2$  and bars number  $q_2$  are equal, the current through the bars  $I_b$  is equal with the phase current, number of turns per phase  $w_c = w_2/2$ .

The voltage induced in the rotor bars are equal and between them there are a phase difference  $2\pi p/q_2$ , and for the bar  $k$  can be expressed: [9]

$$e_{2bk} = E_{2b} \sqrt{2} \cos \left[ \omega_2 t - (k-1) \frac{2\pi p}{q_2} \right] \quad (5)$$

The effective voltage value depends on the maximum induction and flux:

$$E_{2b} = \frac{\pi}{\sqrt{2}} f_2 \Phi_m \quad \text{and} \quad \omega_2 = 2\pi f_2 \quad (6)$$

The currents through the bars are:

$$i_{bk} = I_b \sqrt{2} \cos \left[ \omega_2 t - \gamma_2 - (k-1) \frac{2\pi p}{q_2} \right] \quad (7)$$

Considering a loop between two bars and the end rings, the voltage equation in the loop is:

$$R_{b(k-1)} i_{b(k-1)} - R_{bk} i_{bk} + 2R_e i_e + \frac{d\Phi_{rk}}{dt} = 0 \quad (8)$$

Where  $R_b$  is rotor bar resistance,  $R_e$  is end ring resistance,  $\Phi_r$  is the flux induced in the loop. The equivalent circuit model of induction motor with squirrel-cage rotor can be adjusted like in figure 2.

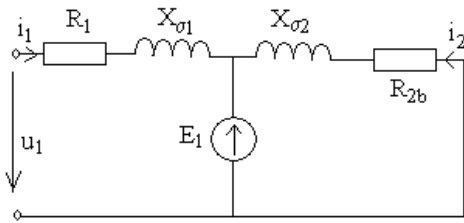


Fig.2. The equivalent circuit for squirrel cage rotor induction motor.

Where  $R_{2b} = R_b/N_b$ ,  $R_e/N_b \ll R_b$ . [13]

#### 4. Broken rotor bar modeling

There are many sources of vibration in induction motors due to electrical and mechanical forces which act during the functioning of the motor. If for some reason an unbalance of these forces appear then a

vibration appears also.

A fault which appears very often is the broken rotor bar or the cracked rotor end rings. This can be caused by different factors like thermal, electrical or mechanical factors. During operation the temperature is high and due to the rotation speed the solderings or a bar can break. [6]

If a rotor bar is broken, no current will flow in the bar and no magnetic field will appear around the bar. The magnetic field and the force in this side will be different from the opposite side and a magnetic unbalance appears whose rotation speed is equal with the rotational speed of the motor and modulates at the frequency which depends on the slip and number of poles. Likewise if a rotor bar has a different parameter, a similar magnetic unbalance appears. Further this change causes more heating in the rotor, the rotor can bend and it creates an eccentric rotor and more unbalance in the magnetic field and force.[11]

To highlight the magnetic field and flux changes around the rotor, equations for the stator and rotor voltage will be written similar to equation (2):

$$\begin{aligned} u_s &= i_s R_s + \frac{d\Phi_s}{dt} \\ u_r &= i_r R_r + \frac{d\Phi_r}{dt} \end{aligned} \quad (9)$$

Where  $u_r = 0$  and the stator and rotor fluxes  $\Phi_s$ ,  $\Phi_r$  include both useful and mutual fluxes which can be expressed as a function of inductances and currents. For one rotor phase the flux is [12]:

$$\begin{aligned} \Phi_{ra} &= M_{sr} \cos(-\theta_m) i_{sA} + M_{sr} \cos \left( -\theta_m + \frac{2\pi}{3} \right) i_{sB} + M_{sr} \cos \left( -\theta_m + \frac{4\pi}{3} \right) i_{sC} + L_r i_{ra} + M_r i_{rb} + M_r i_{rc} \end{aligned} \quad (10)$$

Similar equation can be written for each stator flux. The flux expressions can be written in a simple and compact form highlighting only the stator and rotor inductivities and currents.

$$\begin{aligned} \Phi_s &= L_s i_s + L_m e^{j\alpha} i_r \\ \Phi_r &= L_m e^{-j\alpha} i_s + L_r i_r \end{aligned} \quad (11)$$

From the equations (8) and (10) are deduced the flux and current expressions:

$$\begin{aligned} \frac{d\Phi_s}{dt} &= u_s - i_s R_s \\ \frac{d\Phi_r}{dt} &= u_r - i_r R_r \\ i_s &= \frac{1}{L_s} (\Phi_s - L_m e^{j\alpha} i_r) \\ i_r &= \frac{1}{L_r} (\Phi_r - L_m e^{-j\alpha} i_s) \end{aligned} \quad (12)$$

If  $u_s$ ,  $u_r$  and  $\alpha$  are given, then these equations define the motor currents.

Based on the equivalent circuit from the figure 2 the following equations can be written:

$$\begin{aligned} u_1 &= R_1 i_1 + X_{\sigma 1} \frac{di_1}{dt} - E_1 \\ 0 &= R_{2b} i_2 + X_{\sigma 2} \frac{di_2}{dt} - E_1 \end{aligned} \quad (13)$$

Where  $E_1 = L_m \frac{di_0}{dt}$  and  $i_1 + i_2 = i_0$

Based on equation (13) and using the expression for  $X_{\sigma 1}, X_{\sigma 2}$ , the currents equations are:

$$\begin{aligned} \frac{di_1}{dt} &= \frac{L_m}{L_1-L_m} \frac{di_2}{dt} - \frac{R_1}{L_1-L_m} i_1 + \frac{1}{L_1-L_m} u_1 \\ \frac{di_2}{dt} &= \frac{L_m}{L_2-L_m} \frac{di_1}{dt} - \frac{R_{2b}}{L_2-L_m} i_2 \end{aligned} \quad (14)$$

Using these equations a Simulink model was developed, figure 3.

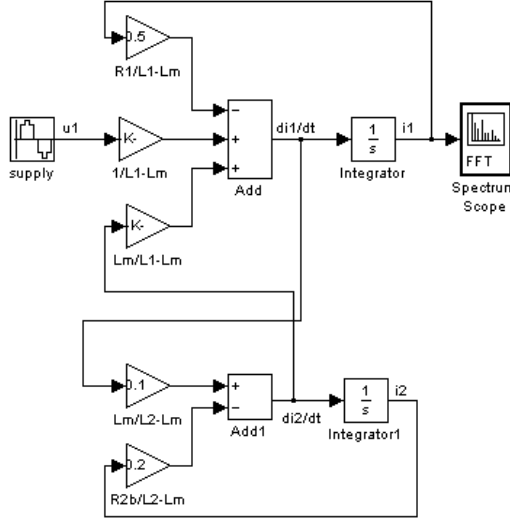


Fig.3. Simulink model of ac motor based on the equivalent circuit.

The matrix form of the (14) equation is:

$$\frac{d}{dt} \begin{bmatrix} i_1 \\ i_2 \end{bmatrix} = \begin{bmatrix} 0 & \frac{L_m}{L_1-L_m} \\ \frac{L_m}{L_2-L_m} & 0 \end{bmatrix} \frac{d}{dt} \begin{bmatrix} i_1 \\ i_2 \end{bmatrix} + \begin{bmatrix} \frac{-R_1}{L_1-L_m} & 0 \\ 0 & \frac{-R_{2b}}{L_2-L_m} \end{bmatrix} \begin{bmatrix} i_1 \\ i_2 \end{bmatrix} + \begin{bmatrix} \frac{1}{L_1-L_m} \\ 0 \end{bmatrix} u_1 \quad (15)$$

For no broken rotor bar the stator current  $i_1$  has theoretically sinusoidal form, no harmonics are present, on the spectrum a single component will appear.

For broken rotor bar changes will occur,  $R_{2b}$  is increasing,  $X_{\sigma 2}$  is decreasing, the rotor current and the flux is changing too. The flux distribution will not be uniform.

This irregularity can be modelled by modifying  $R_{2b}$ ,  $L_2$  and  $L_m$ . Knowing the relationship between the flux and the inductance, they can be described through the same function of variation, which is introduced in the model.

Based on the above the variation of the flux can be estimated through a sinusoidal function with the frequency proportional to the rotational speed of the induction motor. The current induced by this flux variation overlaps with the stator current and appears in the stator current spectrum.

On figure 4 can be observed the sideband frequencies which appears in the stator current spectrum (only the positive side should be considered).

The sideband frequencies appear on the two sides of the base frequency. The base frequency of the stator current is equal to the power supply frequency. The sideband frequencies are very close because the slip is small.

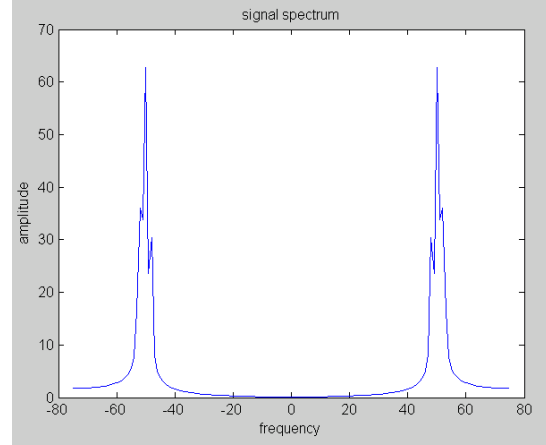


Fig.4. Stator current spectrum for broken rotor bar.

The smaller the slip is, the closer the sideband frequencies are to the basic frequency.

The model and the simulation was done for one phase, for the other two phases the result is similar only there is a phase shift between them.

## 5. Conclusions

Induction motors are a very important part of operation systems so their control and reliability are improving. During operation they may fail due to different factors. The sooner the faults are detected, the faster can one intervene to solve the problem and reduce the losses. Using the proper fault detection techniques the problems can be solved in time.

One of the fault detection techniques is the motor current signature analysis (MCSA) in which the phase current of the electrical motor's stator and/or rotor is measured. The MCSA techniques can be used to detect certain faults between them being broken bar too.

The induction motor voltage equations and equivalent circuit was studied to show the similarities between the squirrel-cage rotor and winding rotor in order to develop an equivalent circuit for the squirrel-cage rotor induction motor. In this equivalent circuit appear the number of rotor bar, resistance of the bars and of the end rings.

Based on the equivalent circuit and voltage and current equations a Simulink model was developed and through this was shown the influence of the broken rotor bar, and the flux distribution modification around the rotor on the stator current. Because the rotor's rotation speed is smaller than the speed of synchronism, the modified flux distribution will have the same frequency as the rotor (different from the

stator flux) and it will induce voltage in stator windings, and current harmonics will appear.

The flux modification was introduced in the model and the appearance of the sideband frequencies was shown. This sideband frequency depends on the slip. This technique is indicated for large induction motors where the slip is larger.

## References

- [1] V. Venkatasubramanian, R. Rengaswamy, K. Yin, S. N. Kavuri, (2003) *A review of process fault detection and diagnosis. Part I: Quantitative model-based methods*, Computers and Chemical Engineering 27, [www.elsevier.com/locate/compchemeng](http://www.elsevier.com/locate/compchemeng)
- [2] *Beginner's guide to machine Vibration*. (2006) Commtest Instruments Ltd., Available on [www.commtest.com](http://www.commtest.com)
- [3] A. Giantomassi, S. Iarlori, S. Longhi, (2014) *Electric Motor Fault Detection and Diagnosis by Kernel Density Estimation and Kullback-Leibler Divergence based on Stator Current Measurements*, IEEE Transactions on Industrial Electronics, January, <https://www.researchgate.net/publication/264235282>
- [4] J. Cusido, J. A. Ortega, J. R. Garcia, L. Romeral, (2006) *New fault detection techniques for induction motors*, Electrical Power Quality and Utilization Magazine vol.II, no.1, <https://www.researchgate.net/>
- [5] W.T. Thomson, P.Orpin, (2002) *Current and vibration monitoring for fault diagnosis and root cause analysis of induction motor drives*, Proceedings of the Thirty-first Turbomachinery Symposium pag.61-68 <https://pdfs.semanticscholar.org/>
- [6] D. M. Sonje, R. K. Munje, (2011) *Rotor Cage Fault Detection in Induction Motors by Motor Current Signature Analysis*, International Conference in Computational Intelligence (ICCI) 2011 Proceedings published in International Journal of Computer Applications@ (IJCA), pag. 22-26, <https://www.researchgate.net/>
- [7] *Mathematical Modeling of Induction Motors*, [https://shodhganga.inflibnet.ac.in/bitstream/10603/4510/12/12\\_chapter%203.pdf](https://shodhganga.inflibnet.ac.in/bitstream/10603/4510/12/12_chapter%203.pdf)
- [8] A. Simion, L. Livadaru, A. Munteanu, (2012) *Mathematical Model of the Three-Phase Induction Machine for the Study of Steady-State and Transient Duty Under Balanced and Unbalanced States*, <http://dx.doi.org/10.5772/49983>
- [9] M.Gogu, (2012) *Masina asincrona*, (Online) Available on [http://www.mircea-gogu.ro/pdf/Curs%20Masini%20electrice/capitolul\\_V.pdf](http://www.mircea-gogu.ro/pdf/Curs%20Masini%20electrice/capitolul_V.pdf)
- [10] M.Morega, (2007) *Maşini şi acţionăre electrice*, Universitatea "Politehnica" Bucuresti,
- [11] W.R.Finley, M.M.Hodowanec, W.G.Holter, (2011) *An Analytical Approach to Solving Motor Vibration Problems*, Siemens Energy & Automation Inc., <https://ieeexplore.ieee.org/document/871297>
- [12] *Induction Motor Model. Generalities*, (2004) <https://www.tdx.cat/bitstream/handle/10803/6317/06Chapter1.PDF?sequence=6&isAllowed=y>
- [13] S. Bachir, S. Tnani, G. Champenois, J-C. Trigeassou, (2014) *Induction motor modeling of broken rotor bars and fault detection by parameter estimation*, <https://www.researchgate.net/publication/228459830>